Corosolic acid attenuates cardiac fibrosis following myocardial infarction in mice

ZHAO-PENG WANG[1,2], YAN CHE[1,2], HENG ZHOU[1,2], YAN-YAN MENG[1,2], HAI-MING WU[1,2], YA-GE JIN[1,2], QING-QING WU[1,2], SHA-SHA WANG[1,2] and YUAN YUAN[1,2]

[1]Department of Cardiology, Renmin Hospital of Wuhan University;
[2]Hubei Key Laboratory of Metabolic and Chronic Diseases, Renmin Hospital of Wuhan University, Wuhan, Hubei 430060, P.R. China

Received July 11, 2019; Accepted December 6, 2019

DOI: 10.3892/ijmm.2020.4531

Abstract. Corosolic acid (CRA) is a pentacyclic triterpenoid isolated from *Lagerstroemia speciosa*. The aim of the present study was to determine whether CRA reduces cardiac remodelling following myocardial infarction (MI) and to elucidate the underlying mechanisms. C57BL/6J mice were randomly divided into control (PBS-treated) or CRA-treated groups. After 14 days of pre-treatment, the mice were subjected to either sham surgery or permanent ligation of the left anterior descending artery. Following surgery, all animals were treated with PBS or CRA (10 or 20 mg/kg/day) for 4 weeks. After 4 weeks, echocardiographic, haemodynamic, gravimetric, histological and biochemical analyses were conducted. The results revealed that, upon MI, mice with CRA treatment exhibited decreased mortality rates, improved ventricular function and attenuated cardiac fibrosis compared with those in control mice. Furthermore, CRA treatment resulted in reduced oxidative stress, inflammation and apoptosis, as well as inhibited the transforming growth factor β1/Smad signalling pathway activation in cardiac tissue. *In vitro* studies further indicated that inhibition of AMP-activated protein kinase α (AMPKα) reversed the protective effect of CRA. In conclusion, the study revealed that CRA attenuated MI-induced cardiac fibrosis and dysfunction through modulation of inflammation and oxidative stress associated with AMPKα.

Introduction

Cardiac fibrosis is the major pathological process in ventricular remodelling occurring after myocardial infarction (MI), and is characterised by deposition of extracellular matrix proteins and ventricular dysfunction (1). Multiple pathophysiological factors contribute to the process, including the inflammatory response, activation of the renin-angiotensin-aldosterone system, oxidative stress and apoptosis (2,3). Chronic infiltration of inflammatory cells, particularly macrophages, following MI can lead to the formation of scar tissue, and macrophage-secreted transforming growth factor β (TGF-β) is a major molecule involved in fibrosis following MI (4). In addition, experimental evidence has indicated that the increased production of reactive oxygen species (ROS) contributes to myocardial fibrosis occurring after MI (5). ROS from multiple sources participate in this process, including xanthine oxidase, inflammatory cells, mitochondria and NADPH oxidases (Noxs) (6,7). Nox2 and Nox4 were identified as the major sources of ROS in the heart, while Nox2 deficiency has been reported to mitigate angiotensin II-induced cardiac hypertrophy in mice (8). Studies have also demonstrated that Nox2 knockout mice exhibited reduced interstitial fibrosis and improved survival rates in a myocardial-infarction model, when compared with those in the control group (9). An *in vitro* study verified that Nox4 knockdown led to decreased fibronectin and collagen synthesis in cardiac fibroblasts treated with angiotensin II (10). In addition, a large amount of ROS exacerbated apoptosis and inflammatory cell infiltration following MI, thus worsening tissue injury and cardiac fibrosis (11).

Imbalances in the production of ROS and the antioxidant capability of the biological system are also important causes of cardiac dysfunction. AMP-activated protein kinase (AMPK) is a critical regulator of cardiomyocyte energy homeostasis and survival. Activation of AMPK has been reported to display a protective effect in myocardial ischaemia-induced damage. AMPK also suppresses oxidative stress through the activation of nuclear factor erythroid 2-related factor 2 (Nrf2) and haem oxygenase (HO)-1, and ameliorates tissue damage (12,13).

Corosolic acid (CRA) is a triterpenoid compound discovered in numerous medicinal herbs, particularly in *Lagerstroemia speciosa* L. (also known as Banaba). CRA initially attracted much attention for its anti-diabetic function (14), while further studies demonstrated that CRA has more functions, including antitumour (15) and anti-atherosclerotic properties (16). Previous studies have confirmed that CRA inhibits acute inflammation by regulating IRAK-1

Correspondence to: Dr Yuan Yuan, Department of Cardiology, Renmin Hospital of Wuhan University, 238 Jiefang Road, Wuhan, Hubei 430060, P.R. China
E-mail: whuyuanyuan@whu.edu.cn

Key words: corosolic acid, myocardial infarction, reactive oxygen species, AMPKα/Nrf2/HO-1 signalling pathway, cardiac fibrosis

phosphorylation via an NF-κB-independent pathway in macrophages (17). In addition, in endothelial dysfunction, CRA protects mitochondrial function by regulating Drp1 phosphorylation (Ser637) in an AMPK-dependent manner, which contributes to inhibiting Nox2 oxidase signalling and suppressing NLRP3 inflammasome activation (18). However, to the best of our knowledge, the effects of CRA on post-MI remodelling have not been reported to date.

Therefore, in the present study, the aim was to evaluate the effects of CRA on MI induced by coronary artery ligation in mice and to explore the underlying mechanism.

Materials and methods

Animals. All animal experimental protocols were approved by the Animal Care and Use Committee of Renmin Hospital of Wuhan University (Wuhan, China) and were conducted in accordance with the National Institutes of Health (NIH) Guide for the Care and Use of Laboratory Animals. Male C57BL/6J mice (n=120; weight, 23.5-27.5 g; age, 8 weeks) were purchased from the Institute of Laboratory Animal Science, CAMS & PUMC (Beijing, China). The animals were housed at a controlled temperature and humidity under a 12-h light-dark cycle with free access to food and water at the Cardiovascular Research Institute of Wuhan University (Wuhan, China). The animals were allowed to acclimatize to the laboratory environment for at least one week, and were then randomly assigned to the control [phosphate-buffered saline (PBS)-treated] and CRA-treated groups (10 and 20 mg/kg; purity, >98%; Baoji Herbest Bio-Tech Co., Ltd.) (19,20). After 14 days of pre-treatment, the mice were subjected to either sham surgery (sham group) or MI by left anterior descending coronary artery ligation. A total of four groups (n=30) were formed, including: Sham group (PBS-treated), MI group (PBS-treated), MI+CRA 10 group (treated with 10 mg/kg CRA), and MI+CRA 20 group (treated with 20 mg/kg CRA). Following surgery, all animals were treated with PBS or CRA for 4 weeks. In the sham, MI, MI+CRA 10 and MI+CRA 20 groups, the number of surviving mice were 30, 15, 22 and 24, respectively at 4 weeks after surgery.

Induction of MI. Briefly, the mice were intraperitoneally anaesthetised with sodium pentobarbital (60 mg/kg), intubated and ventilated with a ventilator. Following a left thoracotomy, the heart was rapidly exposed, and the left anterior descending branch of the coronary artery was quickly identified approximately 2-3 mm away from the inferior margin of the left auricle and ligated with a 7-0 silk suture. In sham-operated mice, the left coronary artery was encircled without ligation. Subsequent to the surgery, all animals were treated with PBS or CRA for 4 weeks.

Echocardiography and haemodynamic analysis. At 4 weeks after surgery, the mice were anaesthetised by inhalation of 1.5-2% isoflurane. Echocardiography was performed to evaluate the function of the left ventricle using a MyLab 30CV system (Biosound Esaote, Inc.) equipped with a 15-MHz probe. M-mode tracings derived from the short axis of the left ventricle at the level of the papillary muscles were recorded. For haemodynamic analysis, insertion of a 1.4-French catheter-tip micromanometer catheter (Millar Instruments) into the left ventricle via the right carotid artery was performed. The heart rates, pressure and volume signals were continuously recorded using an Aria pressure-volume conductance system (Millar Instruments) coupled with a PowerLab/4SP A/D converter. According to the guidelines of the Chinese Animal Welfare Committee, subsequent to pressure-volume measurement, the mice were anaesthetised with 1.5% pentobarbital sodium (60 mg/kg) and then sacrificed by cervical dislocation under anaesthesia.

Injury regions. According to a previous study (21), the heart was described as infarct zone (left ventricle free wall), border zone (left ventricle anterior and posterior walls) and distal zone (interventricular septum). Western blotting and reverse transcription-quantitative PCR (RT-qPCR) were studied using border zone tissue.

Histology. The hearts were removed from the mice, arrested in diastole with 10% KCl, weighed and fixed with 4% formaldehyde, followed by embedding in paraffin. The mouse hearts were cut transversely close to the apex to visualize the left and right ventricles. Tissue sections (4-5 μm) were stained with haematoxylin and eosin (H&E) to assess the infarct size, or stained with picrosirius red (PSR) and Masson's trichrome to assess the collagen accumulation as an indication of fibrosis. The ratio of interstitial fibrosis to the total left ventricular area was calculated based on the examination of 10 microscopic fields that were randomly selected in three individual sections per heart, and the images were further analysed by Image Pro Plus software (version 6.0; Media Cybernetics, Inc.).

After dewaxing and sequentially deparaffinised, tissue sections were stained with haematoxylin for 5 min at room temperature and then moved into differentiation fluid (1% hydrochloric acid alcohol) for 3 sec. After washing with flowing water for 15 min, sections were placed in eosin liquid for 2 min, and then washed with water for 1 min. Finally, sections were washed in graded alcohol (75, 90 and 100%) and dehydrated with xylene 3 times for 5 min each time at room temperature, and covered by the coverslips. For PSR straining, previous steps up to stained into haematoxylin were the same as H&E staining, and the slides were then immersed in 2% phosphomolybdic acid for 2 min, before covering sections in picro-sirius red solution and incubating for 90 min at room temperature. Finally, sections were washed with acetic acid solution for 2 sec, dehydrated, cleared and covered by the coverslips. For the Masson's trichrome staining, after dewaxing, the paraffin sections were transferred from the PBS directly in iron hematoxylin for 8 min at room temperature, rinsed for 1-3 sec in 1% hydrochloric acid alcohol, followed by washing with running tap water for 5 min. Following incubation with 1% Acid Ponceau Fuchsin for 20 min, slides were rinsed in distilled water 5 times. Sections were then placed in 1% Phosphormolybdenic acid for 4 min, and then 2% Anilinblue for 5 min, distilled water for 5 min and then 0.2% Acetic Acid for 2 min. Finally, sections were washed with acetic acid solution, dehydrated, cleared and covered by the coverslips.

Immunohistochemistry. Paraffin-embedded heart sections were sequentially deparaffinised and blocked with 10% normal

goat serum in Tris-buffered saline with 1% bovine serum albumin at 37˚C for 2 h. The sections were incubated overnight at 4˚C with primary antibodies against Nox4 (1:200; Abcam; ab154244), HO-1 (1:200; Abcam; ab13243) and $CD68^+$ (1:200; Abcam; ab125212), followed by incubation with EnVision™+/HRP reagent at 37˚C for 1 h, and staining with a DAB detection kit (GK600710; Gene Tech). Images of stained cells were captured with a light optical microscope at x400 magnification.

Western blot analysis. The ventricular tissues were homogenised by a lapping machine and lysed in RIPA lysis buffer. The protein lysates were collected, and the protein concentration was measured with a BCA kit (Synergy HT; BioTek Instruments, Inc.). Next, protein lysates were separated by SDS-PAGE (10% gel) and transferred onto Immobilon-PL transfer membranes (Millipore). The membranes were blocked with 5% skim milk and then incubated overnight at 4˚C with the following primary antibodies: Nox2 (1:1,000; ab129068), Nox4 (1:1,000; ab154244), HO-1 (1:1,000; ab13243), Nrf2 (1:1,000; ab31163), TGFβ1 (1:1,000; ab64715), monocyte chemotactic protein 1 (1:1,000; Mcp-1; ab151538), C-C chemokine receptor type 2 (1:1,000; CCR2; ab203128), P-inhibitor of NF-κB kinase β (1:1,000; P-Ikkβ; ab59195) and T-Ikkβ (1:1,000; ab178870), which were purchased from Abcam; P-AMPKα (1:1,000; 2535), T-AMPKα (1:1,000; 2603P), B-cell lymphoma 2 (1:1,000; Bcl2; 2870), Bcl2-associated X protein (1:1,000; Bax; 2772), T-p65 (1:1,000; 8242), P-Smad2 (1:1,000; 3108S), T-Smad2 (1:1,000; 3103s), P-Smad3 (1:1,000; 8769), T-Smad3 (1:1,000; 9513s) and GAPDH (1:1,000; 2118), which were obtained from Cell Signaling Technology, Inc.; and P-p65 (1:1,000; s276; cat. no. BS4135), obtained from Bioworld Technology, Inc. The samples were subsequently incubated with the goat anti-mouse IgG (P/N 925-32210; 1:1,250; LI-COR Biosciences) and goat anti-rabbit IgG (P/N 925-32211; 1:1,250; LI-COR Biosciences) for 1 h at room temperature. (Thermo Fisher Scientific, Inc.). Next, the membranes were incubated with enhanced chemiluminescence reagent (HP193406; Wuhan Servicebio Technology). Finally, the blots were scanned using a ChemiDoc Imaging System (cat. no. 733BR2234; Bio-Rad Laboratories, Inc.) and analysed using ImageJ software (NIH).

RT-qPCR. The relative mRNA expression levels of atrial natriuretic peptide (ANP), B-type natriuretic peptide (BNP), α-myosin heavy chain (α-MHC), β-MHC, connective tissue growth factor (CTGF), Collagen I α1, Collagen III α1, fibronectin, Nox4, Nox2, HO-1, interleukin-1β (IL-1β), tumour necrosis factor α (TNF-α) and IL-6 were determined by RT-qPCR. Briefly, total RNA was isolated from the snap-frozen tissues and cardiomyocytes using an RNA isolation kit (15596-026; Invitrogen; Thermo Fisher Scientific, Inc.). The yield and purity of RNA samples were calculated spectrophotometrically according to the A260/A280 and A230/260 ratios using a SmartSpec Plus spectrophotometer (Bio-Rad Laboratories, Inc.). Next, RNA (2 μg of each sample) was reverse transcribed into cDNA using oligo(dT) primers and the Transcriptor First Strand cDNA Synthesis kit (4897030001; Roche). PCR amplifications were performed using a LightCycler 480 SYBR-Green I Master Mix (04887352001; Roche). All PCR primers are listed in Table SI. The thermal profile consisted of 10 min of pre-incubation step at 95˚C for FastStart Taq DNA polymerase activation, followed by 45 cycles of PCR at 95˚C for 10 sec (denaturation), 60˚C for 20 sec (annealing), and 72˚C for 30 sec (elongation). Amplified cDNA products were detected by melting curve analysis which consisted of 95˚C for 5 sec and 65˚C for 1 min, and heated to 97˚C to detect continuous changes in fluorescence of SYBR-Green I. After 45 cycles, the housekeeping gene GAPDH was used to normalize the gene expression (22).

Cell culture. H9C2 cells were cultured in Dulbecco's modified Eagle medium containing 10% foetal bovine serum (FBS) with streptomycin (100 mg/ml) and penicillin (100 U/ml) under standard conditions at 37˚C with 5% CO_2. Cells in exponential growth were dissociated with 0.25% trypsin (Gibco; Thermo Fisher Scientific, Inc.) and seeded in 6-well or 24-well culture plates at a density of $1x10^5$ cells/ml prior to incubation for 24 h. Next, different concentrations of CRA were added to the medium 1 h before hypoxia injury. Among the five CRA concentrations tested (0.1, 1, 5, 10 and 20 μM), the H9C2 cells in the 0.1 and 20 μM-treated groups are in poor condition under hypoxia, thus only three CRA concentrations were selected for this analysis, including 1, 5 and 10 μM (data not shown). For the induction of hypoxia injury, the cells were cultured in D-Hank's solution in an MCO-18M O_2/CO_2 incubator (Sanyo Electric Co., Ltd.) with 1% O_2, 5% CO_2 and 94% N_2 for 24 h. Oxidative stress was detected by western blotting, PCR and ROS detection, and apoptosis was detected by TUNEL assay.

Transfection experiment. H9c2 cells were transfected with 50 μg AMPK α2 siRNA (GCCCAGATGAACGCTAAGATA) or 50 μg control siRNA; (Guangzhou RiboBio Co. Ltd.) and Lipo6000™ (Beyotime Institute of Biotechnology) according to the manufacturer's protocol. Briefly, DMEM (Gibco; Thermo Fisher Scientific, Inc.) medium without serum and Lipo6000 were mixed in a PE tube for 5 min, AMPK α2 siRNA (50 μM) and DMEM medium without serum were mixed in another PE tube for 5 min, and the two PE tubes were evenly mixed into another PE tube. After 5 min, they were added to a 6-well plate or a 24-well plate. After 6 h, the medium was replaced and the culture continued for 48 h under standard conditions at 37˚C with 5% CO_2.

ROS detection. 2,7-Dichlorodihydrofluorescein diacetate (DCFH-DA; Invitrogen; Thermo Fisher Scientific, Inc.) was used to detect the ROS levels in H9C2 cells following treatment and hypoxia. Briefly, the cells were cultured in 24-well plates with or without CRA, and then exposed to hypoxia for 24 h. Next, the cells were incubated with DCFH-DA for 30 min at 37˚C. The production of ROS by the cells was observed under an Olympus IX53 fluorescence microscope (Olympus Corporation).

TUNEL assay. Apoptotic cells and heart tissue sections were detected by TUNEL straining according to the manufacturer's instructions (S7111; EMD Millipore Crop). For cells, they were fixed with 4% paraformaldehyde in 4˚C overnight, rinsed with PBS and then incubated in 0.1% Triton X-100 for 5 min at room temperature. For tissue sections, after routinely

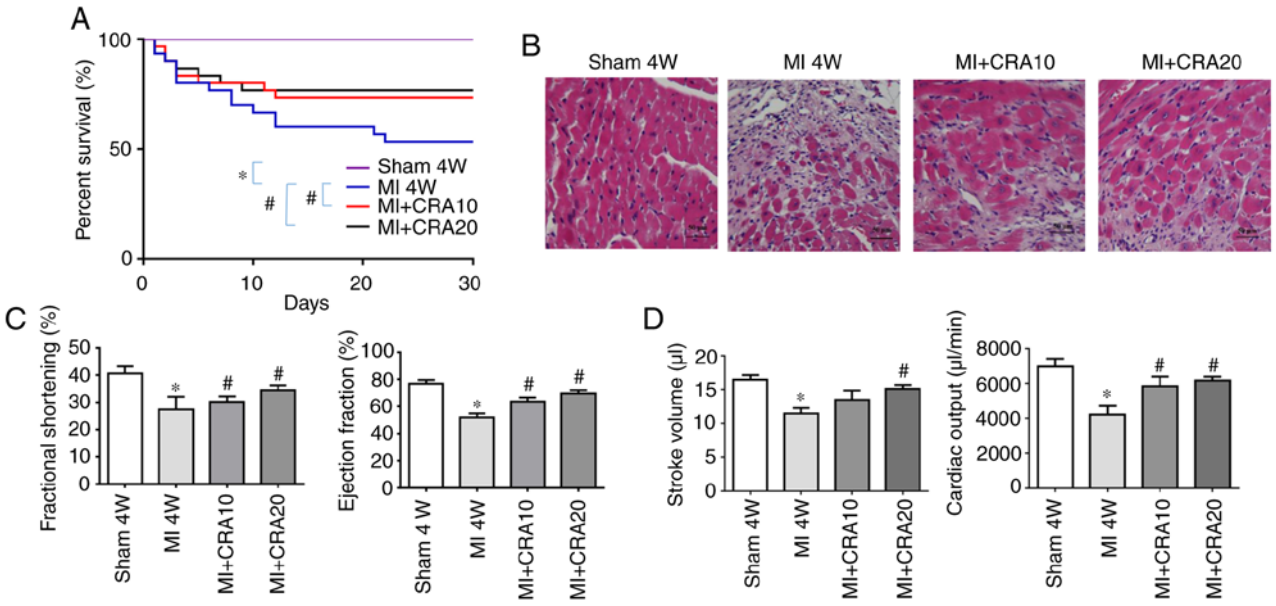

Figure 1. Effects of CRA on cardiac dysfunction following MI. (A) Changes in the survival rates of mice following MI (n=30). (B) Haematoxylin and eosin straining results at 4 weeks after MI (magnification, x200). (C) Echocardiographic analysis of mice at 4 weeks after sham surgery or MI induction, showing the percentages of fractional shortening and ejection fraction (n=10). (D) Hemodynamic analysis of stroke work and cardiac output at 4 weeks after MI (n=10). *P<0.05 vs. sham group; #P<0.05 vs. the MI group. CRA, corosolic acid; MI, myocardial infarction.

dewaxing and hydration, TUNEL straining was performed according to the protocols provided with each kit. Briefly, equilibration of buffer (EMD Millipore Corp.) was added to cells or tissue sections and incubated for 10 sec at room temperature, the TDT Enzyme (EMD Millipore Corp.) was added to the cells or tissue sections and incubated for 1 h at 37˚C in a dark humidified chamber. Stop/Wash buffer (EMD Millipore Corp.) was added and incubated for 10 min at room temperature, rinsed with PBS before Anti-Digoxigenin Fluorescein (EMD Millipore Corp.) was added, and then incubated for 30 min at room temperature in a dark humidified chamber. Finally, stained with 4', 6-diamidino-2'-phenylindole dihydrochloride (DAPI) (Invitrogen; Thermo Fisher Scientific, Inc.) before washed by PBS. Cells were detected using a fluorescence microscope at x200 magnification, and the ratio of TUNEL-positive cells to total cells was calculated after at least 20 viewed fields.

Statistical analysis. The data are presented as the mean ± standard error of the mean. Data were analysed with a one-way analysis of variance followed by a post-hoc Tukey's test using SPSS software (version 22.0; SPSS, Inc.). A value of P<0.05 was considered to denote a statistically significant difference.

Results

CRA improves the survival rates and post-infarction cardiac function of mice. The survival rates of mice in the MI+CRA 10 and MI+CRA 20 groups were significantly higher in comparison with those in the MI group (Fig. 1A). H&E staining revealed that the CRA-treated groups displayed a higher number of cardiomyocytes and reduced infarct size in the border zone at 4 weeks after MI, as shown in Fig. 1B. Echocardiography analysis demonstrated that CRA treatment improved the left ventricular function of mice after MI, as evidenced by increased fractional shortening, ejection fraction, stroke work and cardiac output compared with the untreated MI group (Fig. 1C and D).

CRA attenuates cardiac fibrosis. To explore whether CRA affects cardiac fibrosis following MI, PSR staining (Fig. 2A) and Masson's trichrome staining (Fig. S1) were performed. It was observed that CRA decreased the interstitial fibrosis caused by MI. Additionally, CRA increased the transcription of α-MHC, and inhibited the transcription of hypertrophic markers (ANP, BNP, and β-MHC) and fibrotic markers (CTGF, Collagen Iα, Collagen IIIα and FN) at 4 weeks after MI, as compared with the untreated MI group (Fig. 2B). These data indicated that CRA treatment alleviated the cardiac remodelling following MI.

CRA reverses MI-induced inactivation of the AMPKα/Nrf2/HO-1 signalling pathway and attenuates oxidative stress. Nox-mediated oxidative stress serves a significant role in the progression of myocardial fibrosis (9,11). In the present study, H9C2 cells were exposed to hypoxia (1% O_2) for 24 h with or without CRA treatment. Western blot analysis revealed that Nox2, HO-1 and Nox4 were upregulated in hypoxia-induced cardiomyocytes. However, CRA treatment inhibited the expression levels of Nox2 and Nox4 proteins, while it increased HO-1 expression in the hypoxia-induced cardiomyocytes (Fig. 3A). RT-qPCR data confirmed that CRA pre-treatment led to reduced mRNA expression levels of Nox2 and Nox4, and higher mRNA expression levels of HO-1 (Fig. 3B). Furthermore, as shown in Fig. 3C, immunohistochemical analysis indicated that CRA treatment evidently increased HO-1 and decreased Nox4 expression following MI. Consistently, *in vivo* studies indicated that CRA decreased the expression levels of Nox2 and Nox4, and increased HO-1 expression in myocardial tissue after 4 weeks of MI (Fig. 3D).

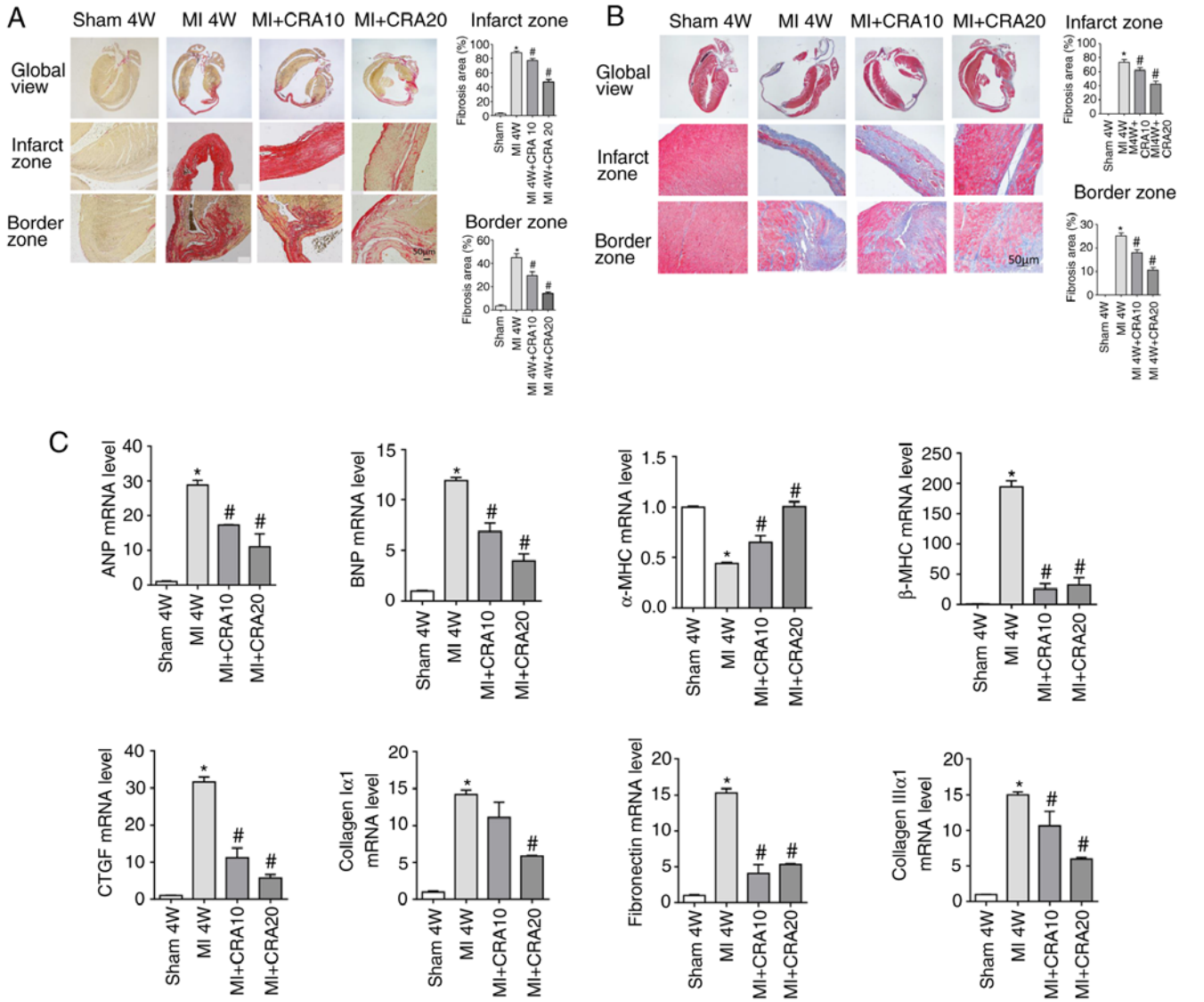

Figure 2. Effects of CRA on cardiac fibrosis following MI. (A) Picrosirius red staining of histological sections at 4 weeks after MI (magnification, x100; n=5). (B) Masson's' trichrome staining of histological sections at 4 weeks after MI (magnification: x100) (n=5). (C) Reverse transcription-quantitative polymerase chain reaction analyses of ANP, BNP, α-SMA, β-MHC, CTGF, Collagen I α1, Collagen III α1 and fibronectin (n=6). *P<0.05 vs. sham group; #P<0.05 vs. MI group. CRA, corosolic acid; MI, myocardial infarction; ANP, atrial natriuretic peptide; BNP, B-type natriuretic peptide; MHC, myosin heavy chain; CTGF, connective tissue growth factor.

In order to identify the underlying mechanism of the effect of CRA, proteins associated with the signalling pathways involved in oxidative stress were also detected in the myocardial tissues. It was observed that MI-induced inactivation of AMPKα/Nrf2/HO-1 signalling was reversed by CRA treatment (Fig. 3D).

CRA regulates the TGF-β1/Smad signalling pathway and reduces the infiltration of macrophages in vivo. The TGF-β1/Smad signalling pathway is known to serve a crucial role in the pathogenesis of numerous fibrotic diseases, and thus the TGF-β1/Smad cascade activation was tested in the current study. As shown in Fig. 4A, the MI-induced increase in the protein levels of TGF-β1, P-Smad2 and P-Smad3 was attenuated in CRA-treated mice (Fig. 4A). Since macrophage-secreted TGF-β is a major molecule involved in fibrosis after MI, the infiltration of macrophages in the myocardial tissues of each group was then examined. The Mcp-1 and CCR2 expression levels decreased in the MI+CRA 10 and MI+CRA 20 groups, as compared with those in the untreated MI group (Fig. 4B). In addition, immunohistochemical staining for CD68 in the infarct and border zones revealed decreased macrophage infiltration in CRA-treated hearts post-MI as compared with that observed in the MI alone group (Fig. 4C; IgG negative control staining is shown in Fig. S2).

CRA inhibits inflammation and apoptosis in myocardial tissues. The expression levels of several inflammatory markers, including IL-1β, TNF-α and IL-6, in the myocardial tissues were also detected. As indicated by the RT-qPCR results, CRA decreased the mRNA expression levels of IL-1β, TNF-α and IL-6 in the myocardium post-MI (Fig. 5A), and repressed the expression levels of nuclear transcription factor NF-κB p65 and p-Ikkβ (Fig. 5B). TUNEL assay revealed that MI induced apoptosis, as indicated by the large number of TUNEL-positive cells, while CRA reduced the number of

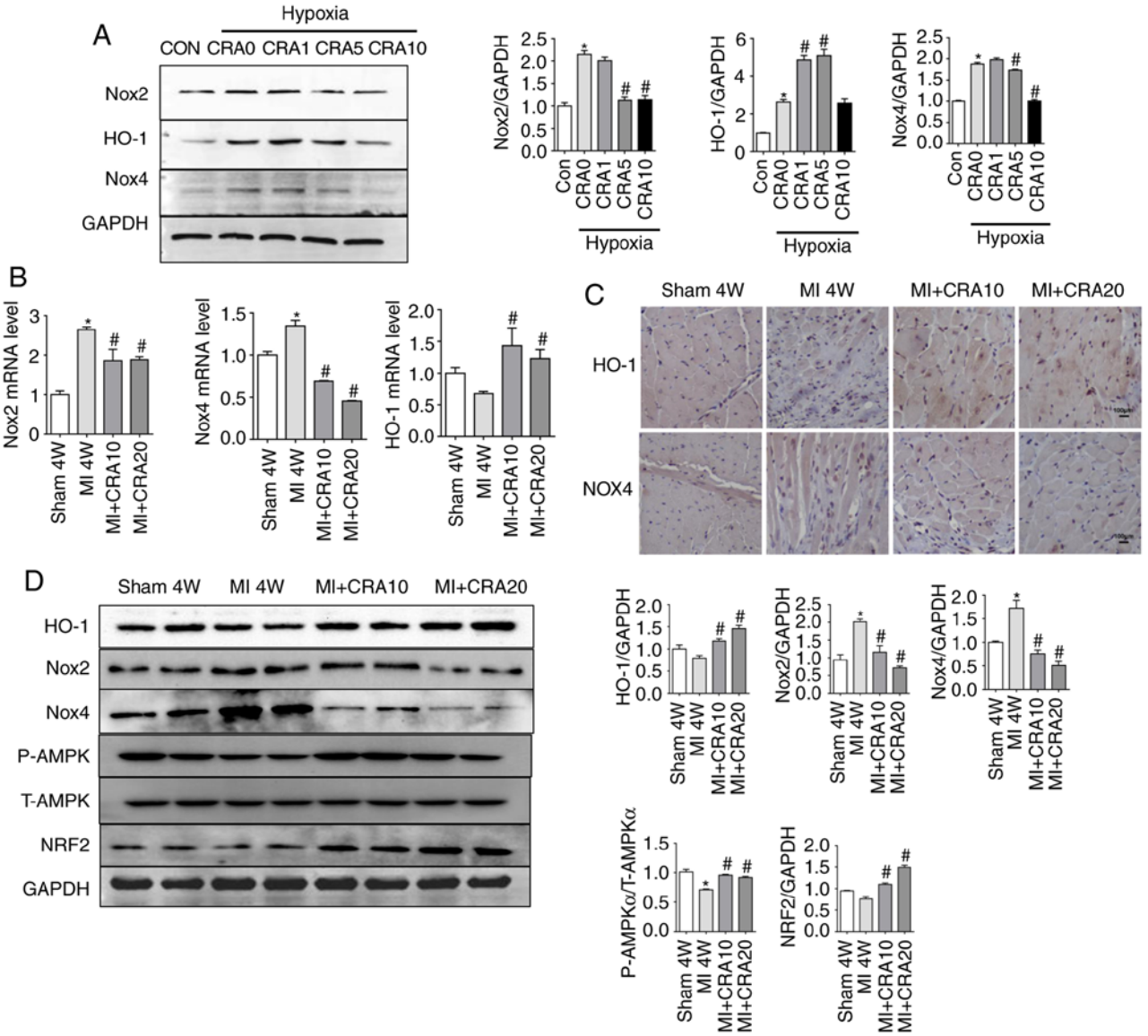

Figure 3. Effects of CRA on oxidative stress following MI. (A) Western blot analysis showing the protein levels of Nox2, HO-1, Nox4 and GAPDH in H9C2 cells treated with hypoxia in the presence or absence of CRA (n=5). *P<0.05 vs. Con group; #P<0.05 vs. hypoxia group. (B) Reverse transcription-quantitative polymerase chain reaction analyses of Nox2, Nox4 and HO-1 mRNA levels in the border zone of cardiac tissues obtained from mice subjected to sham surgery or MI, with or without CRA treatment (n=6). (C) HO-1 and Nox4 expression in the border zone was also examined by immunohistochemistry. (D) Western blot analysis indicating the protein levels of HO-1, Nox2, Nox4, AMPKα, Nrf2 and GAPDH in cardiac tissue (n=5). *P<0.05 vs. sham group; #P<0.05 vs. MI group. CRA, corosolic acid; MI, myocardial infarction; Nox, NADPH oxidase; HO-1, haem oxygenase 1; AMPKα, AMP-activated protein kinase α; Nrf2, nuclear factor erythroid 2-related factor 2.

apoptotic cells (Fig. 5C). Western blot analysis further demonstrated increased expression of the pro-apoptotic protein Bax and decreased expression of the anti-apoptotic protein Bcl-2 in the MI group, while CRA inhibited these MI-induced changes (Fig. 5D).

Inhibition of AMPKα reverses the protective effect of CRA in H9C2 cells. As detected by the DCFH-DA method, CRA treatment partly blocked the hypoxia-induced ROS upregulation in H9C2 cells; however, the antioxidant capacity of CRA was reversed by AMPKα siRNA (Fig. 6A). In addition, the protective effects of CRA against hypoxia-induced changes were reversed by AMPKα siRNA, as indicated by the results of TUNEL staining (Fig. 6B), and Nox2, P-p65, Nrf2 and HO-1 protein expression levels (Fig. 6C). These results suggested that AMPKα may mediate the protective effects of CRA following MI.

Discussion

Fibrosis is the major cause of the deterioration of cardiac function in patients who survive acute MI. Targeting cardiac fibrosis may significantly delay the progression of heart failure and improve the quality of life of patients. In the present study, the following results were observed: i) CRA inhibited cardiac fibrosis and improved left ventricular dysfunction following MI; ii) CRA reduced the production of ROS, which was associated with regulating the activity of the AMPKα/Nrf2/HO-1 signalling pathway and Noxs, particularly Nox2 and Nox4; iii) CRA inhibited inflammation and apoptosis caused by MI;

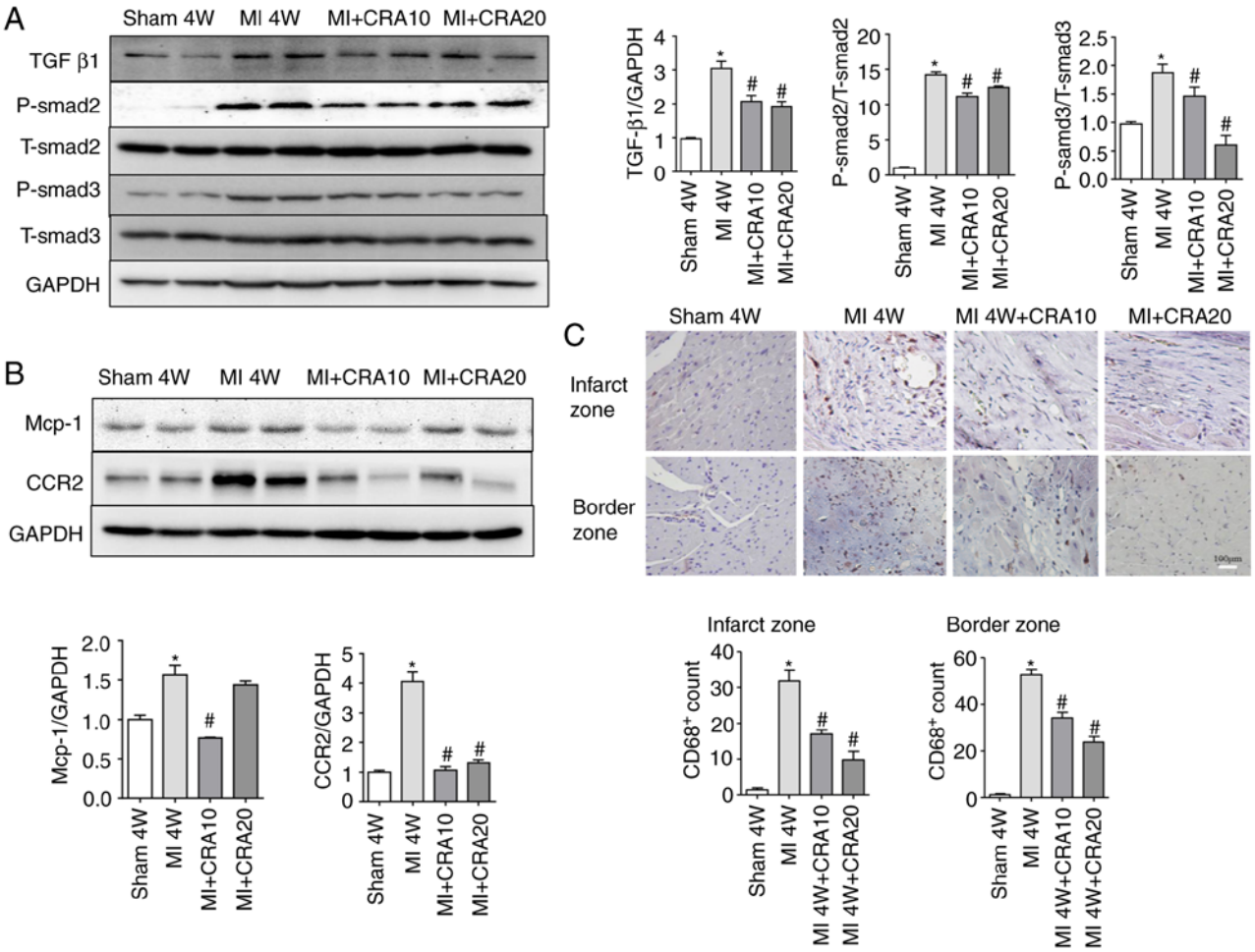

Figure 4. CRA regulates TGF-β1/Smads and macrophage infiltration. (A) Western blot analysis of the protein levels of TGF-β1/Smad signals in cardiac tissue, including TGF-β1, P-Smad2, T-Smad2, P-Smad3, T-Smad3 and GAPDH (n=5). (B) Western blot analysis of the protein levels of Mcp-1, CCR2 and GAPDH in cardiac tissue (n=5). (C) CD68 protein in the infarct and border zones of cardiac tissue was determined by immunohistochemistry (magnification, x200; n=6). *P<0.05 vs. sham group; #P<0.05 vs. MI group. CRA, corosolic acid; MI, myocardial infarction; TGF-β1, transforming growth factor β1; Mcp-1, monocyte chemotactic protein 1; CCR2, C-C chemokine receptor type 2.

and iv) AMPKα inhibition reversed the protective effect of CRA. Collectively, these findings suggest that CRA attenuates MI-induced cardiac fibrosis and dysfunction through modulation of inflammation and oxidative stress associated with AMPKα.

The abnormal deposition of extracellular matrix between non-ischaemic myocardial cells is the main mechanism of fibrosis following MI and is associated with increased mortality (23). It was confirmed that ROS are involved in the synthesis and degradation of collagen (24,25), indicating that oxidative stress serves an important role in synthesis of collagen. It has been reported that Nox2 deficiency attenuates fibrosis and improves left ventricular dysfunction following MI, while inhibition of Nox2 can reduce oxidative stress and apoptosis in hypoxia-induced cells (26). Nox4 is a major source of superoxide (27), and mediates mitochondrial dysfunction and fibronectin synthesis (28). HO-1 is a rate-limiting enzyme in haem degradation and displays a strong protective effect on oxidative damage induced by ROS. The increased expression of HO-1 and the production of bilirubin may regulate the production of endogenous ROS in cells (29). Previous data have also indicated that HO-1 improves mitochondrial damage induced by hypoxia and inhibits the production of Noxs (30). In addition, AMPKα, which is closely associated with cell survival during myocardial ischaemia (31), stimulates Nrf2 and its downstream antioxidant enzyme HO-1 to resist oxidative stress (12). CRA may attenuate cardiac fibrosis by regulating the AMPKα/Nrf2/HO-1/Nox signalling pathway.

In addition to oxidative stress, it has been demonstrated that macrophages are also involved in the process of cardiac fibrosis during MI (32). During the later inflammatory phase of infarct healing, the activity of macrophages is an important cause of fibrosis, while these cells are also an important source of TGF-β following MI (33). In the current study, a decrease in macrophage infiltration was observed in the CRA-treated group, while western blot analysis revealed the downregulation of CCR2 and Mcp-1 following CRA treatment, indicating that CRA attenuated macrophage infiltration through the Mcp-1/CCR2 axis. Previous studies have reported that ROS are associated with the activation of macrophages by participating in the activation of the Mcp-1/CCR2 signalling pathway (34-36). In addition, the current study observed that a high dose of CRA was less effective in blocking Mcp-1 expression, which does not appear to be consistent with the immunohistochemistry results. In fact, there are numerous factors affecting macrophage infiltration in addition to

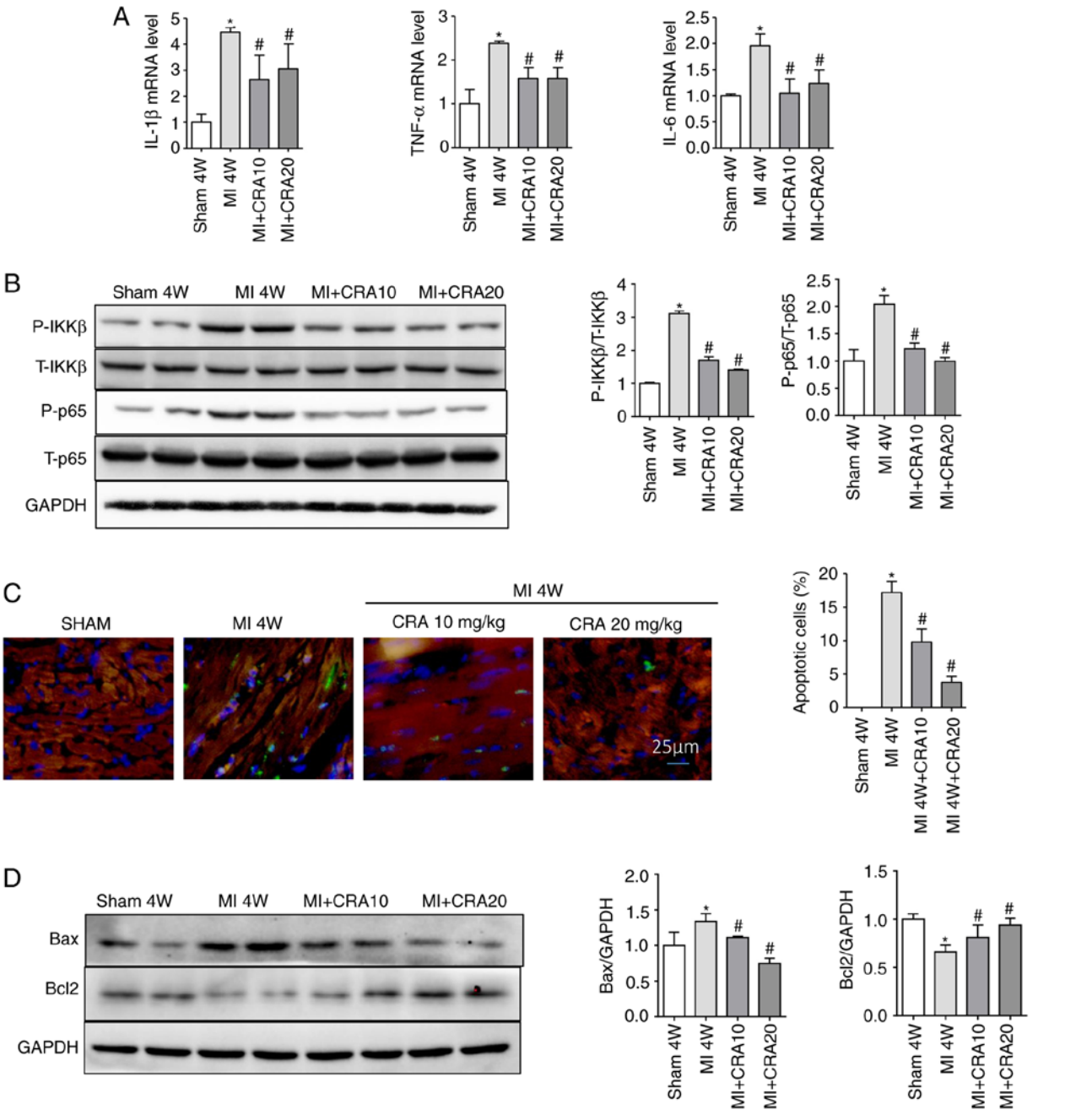

Figure 5. CRA regulates inflammation and apoptosis in cardiac tissues. (A) Reverse transcription-quantitative polymerase chain reaction analyses of IL-1β, TNF-α and IL-6 in border zone of cardiac tissue (n=6). (B) Western blot analysis of the protein levels of p-Ikkβ, T-Ikkβ, p-P65 and T-P65 in border zone tissues (n=5). (C) Representative TUNEL staining of border zone tissues (magnification, x400; n=5). (D) Western blot analysis of the protein levels of Bcl2, Bax and GAPDH in cardiac tissue (n=5). *P<0.05 vs. sham group; #P<0.05 vs. MI group. CRA, corosolic acid; MI, myocardial infarction; IL, interleukin; TNF-α, tumour necrosis factor α; Ikkβ, inhibitor of nuclear factor-κB kinase β; Bcl2, B-cell lymphoma 2; Bax, Bcl2-associated X protein.

Mcp-1, which may account for the discrepancy in the results. Although the blocking effect of high-dose CRA on Mcp-1 was poor, a downward trend was observed. Compared with western blot assay results, the findings of immunohistochemistry may reflect the infiltration of macrophages more intuitively and have more credibility. Therefore, it can be deduced that, although high dose of CRA is less effective in blocking Mcp-1 expression, it still has a strong inhibitory effect on macrophages. Furthermore, previous studies have demonstrated that the anti-inflammatory effect of AMPKα/Nrf2/HO-1 is due to the anti-peroxidation effect and reduced ROS (20,37). Thus, it was hypothesise that the anti-inflammatory ability of CRA may be due to decreased ROS, although further research is needed to verify this hypothesis.

Increased expression of inflammatory cytokines is also an important factor causing apoptosis (38). Apoptosis caused by myocardial ischaemia is one of the reasons for fibrosis and affected cardiac function following MI. Bax and Bcl2 are important regulatory molecules of apoptosis that belong to the Bcl2 family. Bax is located in the cytoplasm and moves to the mitochondria under the stimulation of apoptosis signals, damaging the permeability of the mitochondrial membrane and promoting apoptosis. Furthermore, Bax inhibits the activity of the anti-apoptotic protein Bcl2. In heart failure,

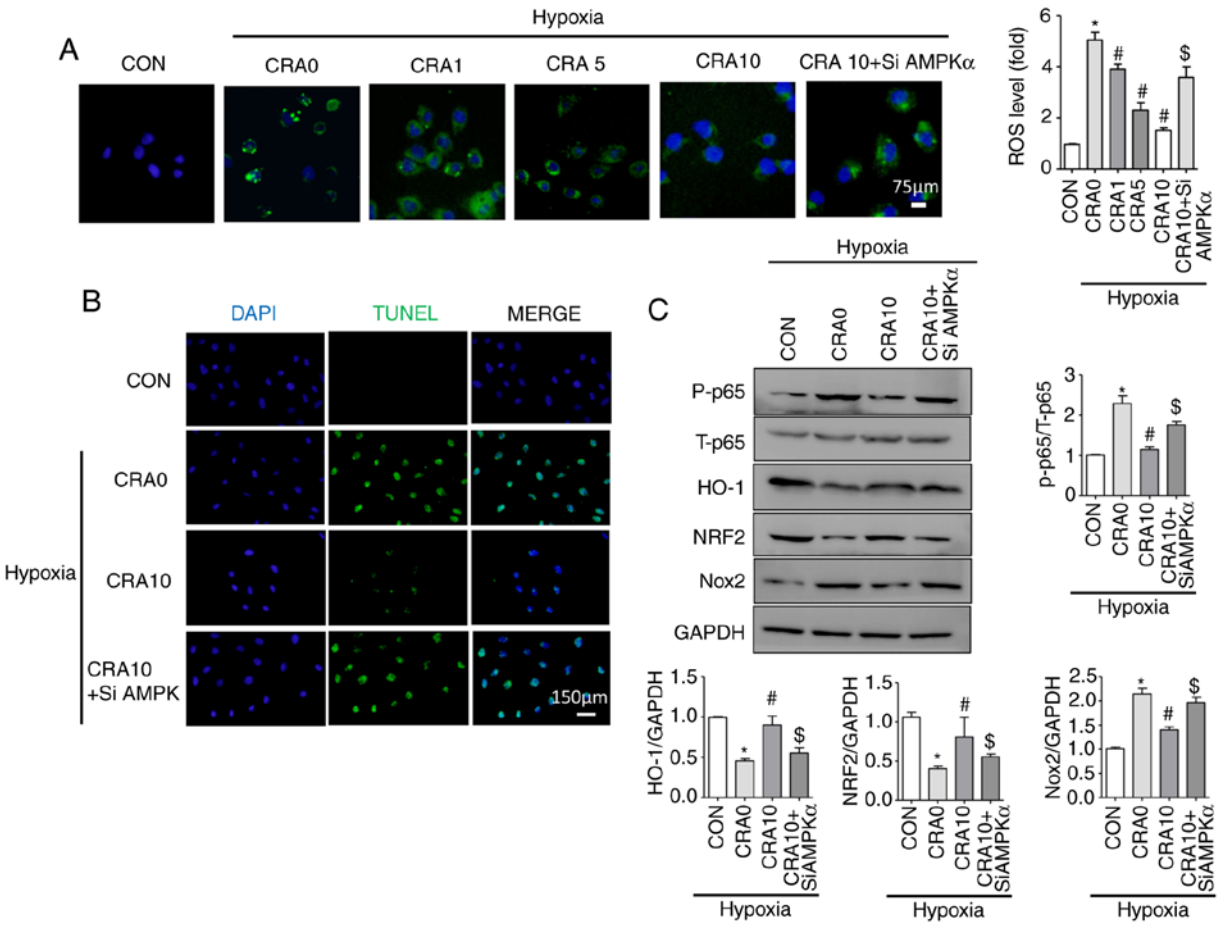

Figure 6. Inhibition of AMPKα reversed the protective effect of CRA against hypoxia in H9C2 cells. (A) ROS production was examined by DCFH-DA staining of H9C2 cells (magnification, x400; n=5). (B) Representative TUNEL staining in H9C2 cells (magnification, x200). (C) Western blot analysis of the protein levels of P-p65, T-p65, HO-1, Nrf2, Nox2 and GAPDH in H9C2 cells (n=5). *P<0.05 vs. CON group; #P<0.05 vs. CRA 0 group; $P<0.05 vs. CRA 10 group. AMPKα, AMP-activated protein kinase α; CRA, corosolic acid; ROS, reactive oxygen species; HO-1, haem oxygenase 1; Nox, NADPH oxidase; Nrf2, nuclear factor erythroid 2-related factor 2; CON, control; siAMPKα, AMPKα siRNA.

the expression of the pro-apoptotic protein Bax in patients is increased (39), while the activity of Bcl2 is decreased; therefore, enhancing the expression of Bcl2 can effectively reduce the occurrence of apoptosis. In the present study, CRA decreased the expression levels of pro-apoptotic protein Bax and increased the activity of anti-apoptotic protein Bcl2 both *in vivo* and *in vitro*, confirming the function of CRA in inhibiting apoptosis of cardiomyocytes.

A previous study revealed that, after 4 weeks of MI, abnormal remodelling occurred in the infarction border zone, accompanied by oxidative stress, inflammation and apoptosis, suggesting that anti-oxidation, anti-apoptotic and anti-inflammatory therapy is an important measure to reduce abnormal remodelling of the border zone (1). The current study attempted to investigate the effect of CRA on ventricular remodelling and heart failure following infarction, and thus the time point of 4 weeks after infarction was selected for investigation. Studies have confirmed that men and women have different risk of cardiovascular disease, which may be associated with metabolism and inflammation (40). To eliminate gender interference in the results, mice of the same sex were selected. However, certain limitations exist in the present study. Firstly, CRA was administered 2 weeks before MI. A previous review on CRA safety reported that using a gel product containing 10 mg CRA can improve the symptoms of patients without causing any adverse effects (41). The current study explored whether CRA can be used as an adjunct drug to improve heart failure in patients with MI or high-risk groups; therefore, prophylactic administration of CRA was provided to the mice. Future studies should verify the effects of CRA on MI when it is only administered to animals following the induction of MI. In addition, the distribution of CRA in the blood following intragastric administration and the proper dosage should be determined in further studies. Finally, whether CRA influences other cell types and signalling pathways in the process of MI requires further investigation.

In conclusion, the data of the present study revealed that CRA attenuated MI-induced cardiac fibrosis and dysfunction through modulation of inflammation, apoptosis and oxidative stress associated with AMPKα. It is, thus, proposed that CRA may be a suitable adjuvant therapy for the treatment of MI and heart failure in clinical practice.

Acknowledgements

The authors would like to thank Professor Tang Qizhu, Renmin Hospital of Wuhan University, for the help and support provided.

Funding

This research was supported by the National Natural Science Foundation of China (grant nos. 81530012 and 81700218), National Key R&D Programme of China (grant no. 2018YFC1311300) and the National Natural Science Foundation of Hubei Province (grant no. 2017CFB320).

Availability of data and materials

The datasets used during the current study are available from the corresponding author upon reasonable request.

Authors' contributions

ZPW and YY designed this study. HZ and YYM performed the data collection. QQW performed the data analysis. YC and YGJ performed the animal experiments. YY and HMW supervised the project and controlled the administration. SSW and HMW performed cell culture; YC wrote the original draft of the manuscript. ZPW and YY reviewed the article. All authors read and approved the final manuscript.

Ethics approval and consent to participate

All animal experimental protocols were approved by the Animal Care and Use Committee of Renmin Hospital of Wuhan University and were conducted in accordance with the National Institutes of Health Guide for the Care and Use of Laboratory Animals.

Patient consent for publication

Not applicable.

Competing interests

The authors declare that they have no competing interests.

References

1. Yang L, Gregorich ZR, Cai W, Zhang P, Young B, Gu Y, Zhang J and Ge Y: Quantitative proteomics and immunohistochemistry reveal insights into cellular and molecular processes in the infarct border zone one month after myocardial infarction. J Proteome Res 16: 2101-2112, 2017.
2. Chen W, Saxena A, Li N, Sun J, Gupta A, Lee DW, Tian Q, Dobaczewski M and Frangogiannis NG: Endogenous IRAK-M attenuates postinfarction remodeling through effects on macrophages and fibroblasts. Arterioscler Thromb Vasc Biol 32: 2598-2608, 2012.
3. Liu X, Wan N, Zhang XJ, Zhao Y, Zhang Y, Hu G, Wan F, Zhang R, Zhu X, Xia H and Li H: Vinexin-β exacerbates cardiac dysfunction post-myocardial infarction via mediating apoptotic and inflammatory responses. Clin Sci (Lond) 128: 923-936, 2015.
4. Bujak M and Frangogiannis NG: The role of TGF-beta signaling in myocardial infarction and cardiac remodeling. Cardiovasc Res 74: 184-195, 2007.
5. Neri M, Fineschi V, Di Paolo M, Pomara C, Riezzo I, Turillazzi E and Cerretani D: Cardiac oxidative stress and inflammatory cytokines response after myocardial infarction. Curr Vasc Pharmacol 13: 26-36, 2015.
6. Lambeth JD: NOX enzymes and the biology of reactive oxygen. Nat Rev Immunol 4: 181-9, 2004.
7. Wilson AJ, Gill EK, Abudalo RA, Edgar KS, Watson CJ and Grieve DJ: Reactive oxygen species signalling in the diabetic heart: Emerging prospect for therapeutic targeting. Heart 104: 293-299, 2018.
8. Byrne JA, Grieve DJ, Bendall JK, Li JM, Gove C, Lambeth JD, Cave AC and Shah AM: Contrasting roles of NADPH oxidase isoforms in pressure-overload versus angiotensin II-induced cardiac hypertrophy. Circ Res 93: 802-805, 2003.
9. Doerries C, Grote K, Hilfiker-Kleiner D, Luchtefeld M, Schaefer A, Holland SM, Sorrentino S, Manes C, Schieffer B, Drexler H and Landmesser U: Critical role of the NAD(P)H oxidase subunit p47phox for left ventricular remodeling/dysfunction and survival after myocardial infarction. Circ Res 100: 894-903, 2007.
10. Somanna NK, Valente AJ, Krenz M, Fay WP, Delafontaine P and Chandrasekar B: The Nox1/4 dual inhibitor GKT137831 or Nox4 knockdown inhibits angiotensin-II-induced adult mouse cardiac fibroblast proliferation and migration. AT1 physically associates with Nox4. J Cell Physiol 231: 1130-1141, 2016.
11. Qi Z, Yin F, Lu L, Shen L, Qi S, Lan L, Luo L and Yin Z: Baicalein reduces lipopolysaccharide-induced inflammation via suppressing JAK/STATs activation and ROS production. Inflamm Res 62: 845-55, 2013.
12. Zhao C, Zhang Y, Liu H, Li P, Zhang H and Cheng G: Fortunellin protects against high fructose-induced diabetic heart injury in mice by suppressing inflammation and oxidative stress via AMPK/Nrf-2 pathway regulation. Biochem Biophys Res Commun 490: 552-559, 2017.
13. Chi PL, Liu CJ, Lee IT, Chen YW, Hsiao LD and Yang CM: HO-1 induction by CO-RM2 attenuates TNF-α-induced cytosolic phospholipase A2 expression via inhibition of PKCα-dependent NADPH oxidase/ROS and NF-kappaB. Mediators Inflamm 2014: 279171, 2014.
14. Miura T, Takagi S and Ishida T: Management of diabetes and its complications with banaba (*Lagerstroemia speciosa* L.) and corosolic acid. Evid Based Complement Alternat Med 2012: 871495, 2012.
15. Kim JH, Kim YH, Song GY, Kim DE, Jeong YJ, Liu KH, Chung YH and Oh S: Ursolic acid and its natural derivative corosolic acid suppress the proliferation of APC-mutated colon cancer cells through promotion of beta-catenin degradation. Food Chem Toxicol 67: 87-95, 2014.
16. Chen H, Yang J, Zhang Q, Chen LH and Wang Q: Corosolic acid ameliorates atherosclerosis in apolipoprotein E-deficient mice by regulating the nuclear factor-κB signaling pathway and inhibiting monocyte chemoattractant protein-1 expression. Circ J 76: 995-1003, 2012.
17. Kim SJ, Cha JY, Kang HS, Lee JH, Lee JY, Park JH, Bae JH, Song DK and Im SS: Corosolic acid ameliorates acute inflammation through inhibition of IRAK-1 phosphorylation in macrophages. BMB Rep 49: 276-281, 2016.
18. Yamaguchi Y, Yamada K, Yoshikawa N, Nakamura K, Haginaka J and Kunitomo M: Corosolic acid prevents oxidative stress, inflammation and hypertension in SHR/NDmcr-cp rats, a model of metabolic syndrome. Life Sci 79: 2474-2479, 2006.
19. Takagi S, Miura T, Ishibashi C, Kawata T, Ishihara E, Gu Y and Ishida T: Effect of corosolic acid on the hydrolysis of disaccharides. J Nutr Sci Vitaminol (Tokyo) 54: 266-8, 2008.
20. Yang J, Leng J, Li JJ, Tang JF, Li Y, Liu BL and Wen XD: Corosolic acid inhibits adipose tissue inflammation and ameliorates insulin resistance via AMPK activation in high-fat fed mice. Phytomedicine 23: 181-190, 2016.
21. Leach JP, Heallen T, Zhang M, Rahmani M, Morikawa Y, Hill MC, Segura A, Willerson JT and Martin JF: Hippo pathway deficiency reverses systolic heart failure after infarction. Nature 550: 260-264, 2017.
22. Fellahi S, El Harrak M, Kuhn JH, Sebbar G, Bouaiti el A, Khataby K, Fihri OF, El Houadfi M and Ennaji MM: Comparison of SYBR green I real-time RT-PCR with conventional agarose gel-based RT-PCR for the diagnosis of infectious bronchitis virus infection in chickens in Morocco. BMC Res Notes 9: 231, 2016.
23. Dobaczewski M, Gonzalez-Quesada C and Frangogiannis NG: The extracellular matrix as a modulator of the inflammatory and reparative response following myocardial infarction. J Mol Cell Cardiol 48: 504-511, 2010.
24. Siwik DA, Pagano PJ and Colucci WS: Oxidative stress regulates collagen synthesis and matrix metalloproteinase activity in cardiac fibroblasts. Am J Physiol Cell Physiol 280: C53-C60, 2001.
25. Kunkemoeller B and Kyriakides TR: Redox signaling in diabetic wound healing regulates extracellular matrix deposition. Antioxid Redox Signal 27: 823-838, 2017.

26. Sirker A, Murdoch CE, Protti A, Sawyer GJ, Santos CX, Martin D, Zhang X, Brewer AC, Zhang M and Shah AM: Cell-specific effects of Nox2 on the acute and chronic response to myocardial infarction. J Mol Cell Cardiol 98: 11-17, 2016.
27. Kuroda J, Ago T, Nishimura A, Nakamura K, Matsuo R, Wakisaka Y, Kamouchi M and Kitazono T: Nox4 is a major source of superoxide production in human brain pericytes. J Vasc Res 51: 429-438, 2014.
28. Ago T, Kuroda J, Pain J, Fu C, Li H and Sadoshima J: Upregulation of Nox4 by hypertrophic stimuli promotes apoptosis and mitochondrial dysfunction in cardiac myocytes. Circ Res 106: 1253-1264, 2010.
29. Cao J, Tsenovoy PL, Thompson EA, Falck JR, Touchon R, Sodhi K, Rezzani R, Shapiro JI and Abraham NG: Agonists of epoxyeicosatrienoic acids reduce infarct size and ameliorate cardiac dysfunction via activation of HO-1 and Wnt1 canonical pathway. Prostaglandins Other Lipid Mediat 116-117: 76-86, 2015.
30. Datla SR, Dusting GJ, Mori TA, Taylor CJ, Croft KD and Jiang F: Induction of heme oxygenase-1 in vivo suppresses NADPH oxidase derived oxidative stress. Hypertension 50: 636-642, 2007.
31. Qi D and Young LH: AMPK: Energy sensor and survival mechanism in the ischemic heart. Trends Endocrinol Metab 26: 422-9, 2015.
32. Yan X, Zhang H, Fan Q, Hu J, Tao R, Chen Q, Iwakura Y, Shen W, Lu L, Zhang Q and Zhang R: Dectin-2 deficiency modulates Th1 differentiation and improves wound healing after myocardial infarction. Circ Res 120: 1116-1129, 2017.
33. Prabhu SD and Frangogiannis NG: The biological basis for cardiac repair after myocardial infarction: From inflammation to fibrosis. Circ Res 119: 91-112, 2016.
34. Ullevig S, Zhao Q, Lee CF, Seok Kim H, Zamora D and Asmis R: NADPH oxidase 4 mediates monocyte priming and accelerated chemotaxis induced by metabolic stress. Arterioscler Thromb Vasc Biol 32: 415-426, 2012.
35. Kim MJ, Kadayat T, Um YJ, Jeong TC, Lee ES and Park PH: Inhibitory effect of 3-(4-Hydroxyphenyl)-1-(thiophen-2-yl) prop-2-en-1-one, a chalcone derivative on MCP-1 expression in macrophages via inhibition of ROS and Akt signaling. Biomol Ther (Seoul) 23: 119-127, 2015.
36. Park SY, Jin ML, Yi EH, Kim Y and Park G: Neochlorogenic acid inhibits against LPS-activated inflammatory responses through up-regulation of Nrf2/HO-1 and involving AMPK pathway. Environ Toxicol Pharmacol 62: 1-10, 2018.
37. Liao HH, Zhu JX, Feng H, Ni J, Zhang N, Chen S, Liu HJ, Yang Z, Deng W and Tang QZ: Myricetin possesses potential protective effects on diabetic cardiomyopathy through inhibiting IκBα/NFκB and enhancing Nrf2/HO-1. Oxid Med Cell Longev 2017: 8370593, 2017.
38. Li M, Ye J, Zhao G, Hong G, Hu X, Cao K, Wu Y and Lu Z: Gas6 attenuates lipopolysaccharideinduced TNFα expression and apoptosis in H9C2 cells through NFkappaB and MAPK inhibition via the Axl/PI3K/Akt pathway. Int J Mol Med 44: 982-994, 2019.
39. Liu W, Ru L, Su C, Qi S and Qi X: Serum levels of inflammatory cytokines and expression of BCL2 and BAX mRNA in peripheral blood mononuclear cells and in patients with chronic heart failure. Med Sci Monit 25: 2633-2639, 2019.
40. Henstridge DC, Abildgaard J, Lindegaard B and Febbraio MA: Metabolic control and sex: A focus on inflammatory-linked mediators. Br J Pharmacol 176: 4193-4207, 2019.
41. Stohs SJ, Miller H and Kaats GR: A review of the efficacy and safety of banaba (*Lagerstroemia speciosa* L.) and corosolic acid. Phytother Res 26: 317-324, 2012.